Double photoionization of the hydrogen molecule from the viewpoint of the time-delay theory

I. A. Ivanov*

Research School of Physics and Engineering, The Australian National University, Canberra ACT 0200, Australia

(Received 17 July 2012; published 28 August 2012)

We studied angular dependency of the time delay in one-photon two-electron photoionization of the hydrogen molecule. Time delay as a function of the angle between velocities of the escaping electrons was shown to have poles at the point corresponding to the kinematic nodes of the reaction. Study of the delay in the vicinity of a pole can provide information about phases of the amplitudes of the reaction.

DOI: 10.1103/PhysRevA.86.023419 PACS number(s): 32.80.Fb, 32.30.Rj, 32.70.−n, 31.15.ve

I. INTRODUCTION

The rapidly developing field of attosecond physics [1] provided a fascinating possibility of experimental study of the details of electron motion in atomic and molecular systems with temporal resolution below characteristic time scales of motion in these systems (typically a hundred attoseconds). Various experimental techniques, such as attosecond streaking [2,3] and angular attosecond streaking [4], have been developed for this purpose. Since the very interpretation of the experimental results relies on the adequate theoretical models, this fast progress in experimental technique goes hand in hand with the development of a theoretical description of the time evolution of the atomic or molecular systems in the presence of electromagnetic field. In the first works on the subject of attosecond streaking the so-called strong field approximation has been used to describe the combined effect of the ultraviolet (UV) and infrared (IR) laser pulses on the system, which is needed to interpret correctly experimental results. This approach has been subsequently refined to include polarization [5,6], and electron correlation effects [7].

This symbiosis of theory and experiment has produced a number of spectacular results, such as an observation of a considerable time delay between photoelectrons emitted from the $2s$ and $2p$ shells in neon [8], or from the hydrogenic $2s$ and $2p$ initial states in He^+ [9]. The time an electron takes to tunnel out in the photoionization event has also been measured [4,10].

In Ref. [11] an approach has been described allowing the so-called complete description of the photoionization process, when not only the traditionally measured modulus of the spectral amplitude but also its phase can be retrieved from the experiment. Information about the phase can be converted into the timing information allowing us to trace experimentally dynamics of the ionization process with attosecond precision. A similar approach has been described in our paper [12].

We describe below a procedure allowing us to obtain phase information for the spectral amplitude of the one-photon two-electron ionization of a hydrogen molecule. This procedure relies on the detailed study of the time delay, a theoretical notion introduced in Ref. [13] for scattering phenomena, and applied subsequently for the photoionization process [14].

*Corresponding author: igor.ivanov@anu.edu.au

II. THEORY AND RESULTS

We solve the time-dependent Schrödinger equation (TDSE) for a hydrogen molecule in the presence of a linearly polarized laser pulse:

$$\boldsymbol{E} = \boldsymbol{E}_0 \sin^2 \frac{\pi t}{T_1} \cos \omega t, \tag{1}$$

with $|\boldsymbol{E}_0| = 0.1$ a.u., $\omega = 75.5$ eV, $T_1 = 4T$, where $T = 2\pi/\omega$ is the optical cycle corresponding to a carrier frequency ω. The laser field is present on the interval of time $(-T_1, T_1)$.

To solve the TDSE we discretized the Hamiltonian operator on a spatial grid $\{r_i\}$. The wave function at the points $\{r_i\}$ is represented as a partial wave expansion:

$$\Psi(\boldsymbol{r}_1, \boldsymbol{r}_2) = \sum_{l_1, l_2, J} f^J_{l_1 l_2}(r_1, r_2) |l_1(1) l_2(2)\ J\rangle, \tag{2}$$

where the notation $|l_1(1) l_2(2)\ J\rangle$ is used for bipolar harmonics [15], and the summation is restricted to $l_1, l_2 = 0$–6, $J = 0$–5. The procedure is described in more details in our paper [16]. The hydrogen molecule at the moment of time $t = -T_1$ is initially in its ground state. The internuclear distance is taken to be equal to its equilibrium value of 0.7414 Å (1.4011 a.u.). We find a solution of the TDSE for the system atom + laser field on the interval $(-T_1, T_1)$. We follow field-free evolution of the system after the end of the laser pulse at $t = T_1$ until $t = 12T$. To solve the TDSE we use the Arnoldi-Lanczos method [17].

To extract from the solution $\Psi(\boldsymbol{r}_1, \boldsymbol{r}_2, t)$ of the TDSE information about the motion of electrons with given asymptotic momenta, we modified the procedure proposed in our work [18], where it was applied for a study of double photoionization of a helium atom.

The wave-packet state $\Psi_{\boldsymbol{k}_1 \boldsymbol{k}_2}(\boldsymbol{r}_1, \boldsymbol{r}_2, t)$ describing two electrons with asymptotic momenta $\boldsymbol{k}_1$, $\boldsymbol{k}_2$ can be obtained by means of a projection operation:

$$\Psi_{\boldsymbol{k}_1 \boldsymbol{k}_2}(\boldsymbol{r}_1, \boldsymbol{r}_2, t) = \hat{P} \Psi(\boldsymbol{r}_1, \boldsymbol{r}_2, t), \tag{3}$$

where the kernel of the projection operator is given by the expression

$$\langle \boldsymbol{r}'_1, \boldsymbol{r}'_2 | \hat{P} | \boldsymbol{r}_1, \boldsymbol{r}_2 \rangle = \int_\Omega \Psi^-_{\boldsymbol{q}_1, \boldsymbol{q}_2}(\boldsymbol{r}_1, \boldsymbol{r}_2) \Psi^-_{\boldsymbol{q}_1, \boldsymbol{q}_2}(\boldsymbol{r}'_1, \boldsymbol{r}'_2)^* d\boldsymbol{q}_1 d\boldsymbol{q}_2, \tag{4}$$

and vectors $\Psi^-_{\boldsymbol{q}_1, \boldsymbol{q}_2}(\boldsymbol{r}_1, \boldsymbol{r}_2)$ are the two-electron scattering states with the ingoing boundary condition. We construct these states using ingoing one-electron scattering states of the H_2^+ ion.

Integration in the momentum space in Eq. (4) is confined to a region centered around the momentum vectors $\boldsymbol{k}_1,\boldsymbol{k}_2$ (specifically $\Omega = \Omega_1 \bigotimes \Omega_2$, where Ω_1 and Ω_2 are balls in momentum space defined by $|\boldsymbol{q}_i - \boldsymbol{k}_i| < 0.25k_i$). Electron density $\rho(\boldsymbol{r},t) = \int |\Psi_{\boldsymbol{k}_1\boldsymbol{k}_2}(\boldsymbol{r},\boldsymbol{r}_1,t)|^2 d\boldsymbol{r}_1$ for such a wave-packet state can be used to visualize motion of two electrons.

We apply this technique below for a particular geometry of the parallel laser field polarization vector and molecular axis. We shall fix the direction of one of the electron momenta ($\boldsymbol{k}_1$) to be parallel to the z axis, and we will study details of electron motion for various directions of the electron momenta $\boldsymbol{k}_2$. Due to the overall cylindrical symmetry of the problem, we can always assume that vector $\boldsymbol{k}_2$ lies in the (x,z) plane. We shall consider the case of the equal energy sharing. For the field frequency that we consider, this corresponds to electron energies $E_1 = E_2 = 12.2$ eV and momenta $k_1 = k_2 = 0.95$ a.u. For these momenta the width of the wave packet obtained using the projection operation defined by Eqs. (3)and (4) is approximately 0.25 a.u. in the momentum space of each electron. Correspondingly, the width in the coordinate space is approximately 4 a.u. Below, for brevity, we shall call the electron moving in the z direction the first electron.

A few consecutive snapshots of the electron motion for this geometry are shown in Fig. 1 for the particular case when a second electron escapes in the direction perpendicular to the z axis.

From the density distributions presented in Fig. 1, one can infer that for large times electron moving in the perpendicular direction is somewhat delayed with respect to the first electron. This respective delay depends strongly on the angle between the momentum vector of the second electron and the z axis. To illustrate this statement we show in Fig. 2 distances from the

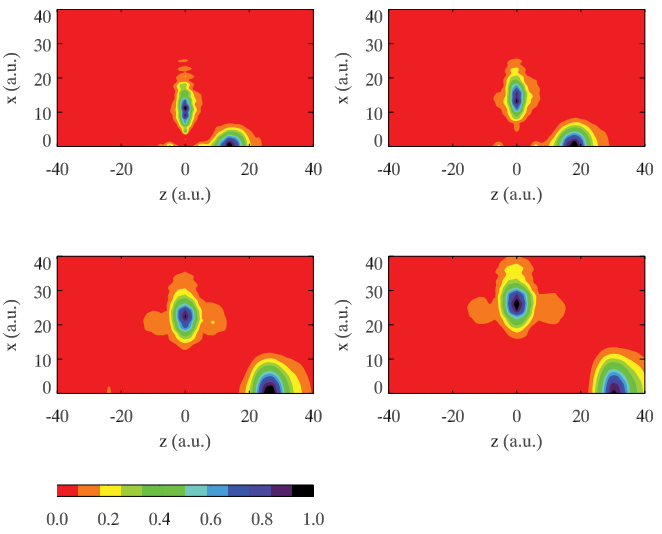

FIG. 1. (Color online) Electron density (normalized so that its maximum value is 1) for the wave-packet state $\Psi_{\boldsymbol{k}_1\boldsymbol{k}_2}(\boldsymbol{r},\boldsymbol{r}_1,t)$ with $\boldsymbol{k}_1$ directed along the molecular axis, $\boldsymbol{k}_2$ in the perpendicular direction. Electrons energies are $E_1 = E_2 = 12.2$ eV. Density is shown for the moments of time $t = 4T$ (upper row, left), $t = 6T$ (upper row, right), $t = 10T$ (second row, left), and $t = 12T$ (second row, right). The color bar (bottom row) indicates the values of the relative density corresponding to different colors.

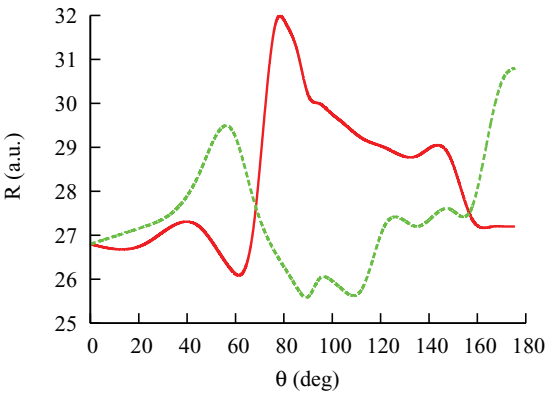

FIG. 2. (Color online) Distance from the origin of the maxima of the density corresponding to the first and second electrons for various angles between $\boldsymbol{k}_2$ and z axis at the moment of time $t = 12T$. First electron (red), solid curve; second electron (green), dashed curve.

origin of the maxima of the density corresponding to the first and second electrons for various angles between $\boldsymbol{k}_2$ and the z axis at the moment of time $t = 12T$.

A puzzling feature one can see from Fig. 2 is a considerable variation of the relative distance between the two electrons with the angle between their momenta, delay of the second electron with respect to the first being especially pronounced for the case of near perpendicular escape geometries. One might argue that the distances of the order of 30 a.u., which electrons have traveled at time $t = 12T$, are not fully asymptotic yet, and it might be that in the truly asymptotic region of large distances, where electrons are detected in the experiment, their relative delay (if any) may be different from that shown in Fig. 2. We can address this question using the time-delay theory [13,14].

The wave-packet state $\Psi_{\boldsymbol{k}_1\boldsymbol{k}_2}(\boldsymbol{r}_1,\boldsymbol{r}_2,t)$ as defined by Eqs. (3) and (4) can be written as

$$\Psi_{\boldsymbol{k}_1\boldsymbol{k}_2}(\boldsymbol{r}_1,\boldsymbol{r}_2,t) = \int d\boldsymbol{q}_1 d\boldsymbol{q}_2 f(\boldsymbol{q}_1,\boldsymbol{q}_2)\Psi^-_{\boldsymbol{q}_1,\boldsymbol{q}_2}(\boldsymbol{r}_1,\boldsymbol{r}_2)e^{-iEt}, \qquad (5)$$

where $E = q_1^2/2 + q_2^2/2$, the amplitudes $f(\boldsymbol{q}_1,\boldsymbol{q}_2)$ can be computed from the TDSE solution $|\Psi(t)\rangle$ as $f(\boldsymbol{q}_1,\boldsymbol{q}_2) = \langle\Psi^-_{\boldsymbol{q}_1,\boldsymbol{q}_2}|\Psi(t)\rangle e^{iEt}$. One can now invoke the well-known chain of arguments relying on the asymptotic properties of the two-electron scattering states and the saddle-point method [8,13,14,19,20]. One easily obtains in this way equations describing for $t \to \infty$ motion of the crests of the wave-packet state $\Psi_{\boldsymbol{k}_1\boldsymbol{k}_2}(\boldsymbol{r}_1,\boldsymbol{r}_2,t)$. These equations for each of the electrons ($i = 1,2$) can be written as

$$\boldsymbol{r}_i(t) \asymp \boldsymbol{k}_i(t - t_{0i}) + \boldsymbol{r}'_i(t). \qquad (6)$$

In Eq. (6) $t_{0i} = d \arg f(\boldsymbol{k}_1,\boldsymbol{k}_2)/dE_i$ are the time delays, functions $\boldsymbol{r}'_i(t)$ are known functions which vary slowly (logarithmically) with t. The important point here is that for the geometry we consider and equal energy sharing $\boldsymbol{r}'_1(t) = \boldsymbol{r}'_2(t)$, so the relative delay of two electrons is determined by the time delays t_{0i}.

Time delays computed as the phase derivatives of the spectral amplitude for various angles between electron momenta

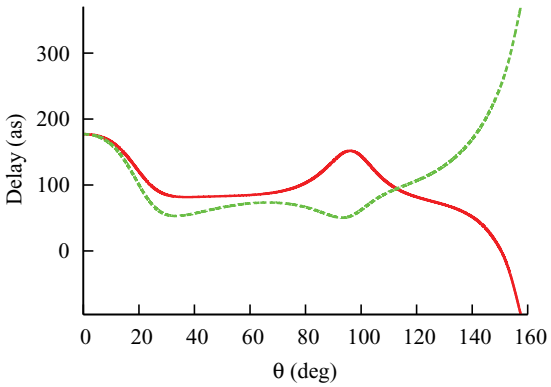

FIG. 3. (Color online) Time delays for various angles between $\boldsymbol{k}_2$ and molecular axis. First electron (green), dashed curve; second electron (red), solid curve.

$\boldsymbol{k}_1$,$\boldsymbol{k}_2$, momentum vector $\boldsymbol{k}_1$ being parallel to the molecular axis, are shown in Fig. 3.

Results presented in Fig. 2 were obtained for modestly large values of radial distances and time, while results shown in Fig. 3 pertain to the asymptotic limit $t \to \infty$. Yet, they tell us very similar stories. For small angles θ between momentum vectors the electrons move in unison. This is an agreement with the expectations based on the well established fact that for small electron energies the dominant mechanism of the two-electron ionization is the knock-out process. In this mechanism the double photoionization proper is viewed as a process in which the first electron ionized by absorbing a photon knocks out the remaining electron in a $(e,2e)$ reaction. For such a process both electrons can be expected to be launched at their respective trajectories at approximately the same time and hence should have similar time delays.

For θ approaching approximately 100° delays for both electrons undergo a fast change. Another apparent feature of the time delays immediately seen from Fig. 3 is the divergent behavior of time delays for angle θ approaching 180°. As we shall see, both these features may provide useful information about the photoionization amplitudes, hardly obtainable by the conventional spectroscopic methods. We shall start with the explanation for the time delay behavior for θ approaching 180°.

The amplitude of the process of the one-photon double ionization can be represented as a sum of symmetric (gerade) and antisymmetric (ungerade) terms [21]. In the vicinity of $\theta \approx 180^\circ$ and for the escape geometry we are using, this representation can be simplified to

$$f(\boldsymbol{q}_1,\boldsymbol{q}_2) = \alpha(E_1,E_2)(1+\cos\theta) + \beta(E_1,E_2), \qquad (7)$$

where $\beta(E_1,E_2)$ is an antisymmetric function of the variables E_1, E_2. For the equal energy sharing this term is therefore zero. We shall need, however, derivatives of the amplitude with respect to energies, and have therefore to preserve the antisymmetric term in the general expression given by Eq. (7). Since $\beta(E_1,E_2)$ is the antisymmetric function of its arguments, it can be represented near the point $E_1 = E_2$ as $\beta(E_1,E_2) \approx \gamma(E_1 - E_2)$. For the time delay of the i-th electron defined in Eq. (6), we obtain after simple algebra the following expression:

$$t_{0i} = a + (-1)^i \frac{b}{1+\cos\theta}, \qquad (8)$$

where $i = 1,2$ for the first and second electron, respectively, and parameters a, b can be expressed in terms of the coefficients introduced above as follows:

$$a = \frac{d\arg\alpha}{dE}, \quad b = \left|\frac{\gamma}{\alpha}\right| \sin(\phi_\gamma - \phi_\alpha). \qquad (9)$$

ϕ_α and ϕ_γ are phases of the amplitudes α and γ, respectively. In Eq. (9) the derivative of $\arg\alpha(E_1,E_2)$ can be taken with respect to any of the arguments, since this function is symmetric. After computing the derivative, all functions are evaluated at the point $E_1 = E_2$ corresponding to the equal energy sharing. The first term in Eq. (8) can be considered as a nonresonance contribution to the time delay, and is the same for both electrons; the second term has a pole at the kinematic node at $\theta = 180^\circ$, coefficients of the pole term having opposite signs for the two electrons. For the angle θ approaching the kinematic node at 180°, time delays for both electrons grow therefore without bound in different directions. This is precisely the sort of behavior seen in Fig. 3. Coefficients of the divergent terms can be obtained from the experiment. So, experimental study of the time delays can, in principle, provide information about the amplitudes in Eq. (8).

To explain the second feature seen in Fig. 3, the sudden fast variation of the time delays in the vicinity of $\theta = 100^\circ$, we studied in more detail the phases of the amplitudes $f(\boldsymbol{q}_1,\boldsymbol{q}_2)$ in Eq. (5). These amplitudes are computed using the solution of the TDSE after the end of the laser pulse. This solution, as represented by Eq. (2), is a sum of partial waves with different total angular momenta J. We can compute separate contributions of each partial wave in Eq. (2). In Fig. 4 we show the thus computed contributions of the partial waves with $J = 1$, $J = 3$, and $J = 5$ to the ionization amplitude $f(\boldsymbol{q}_1,\boldsymbol{q}_2)$.

One can see that something dramatic indeed occurs in the vicinity of $\theta = 100^\circ$. Contributions of the $J = 1$ and $J = 3$ partial waves, which are by far dominating, nearly cancel each other, leading to the rapid variation of the overall phase of the amplitude. That something interesting might be occurring near the point $\theta = 100^\circ$ could be inferred already from the behavior of the triply differential cross sections (TDCSs). TDCSs for this particular geometry and energy sharing have been computed by various methods [16,22–24], all producing very similar results. In our work [16] we employed a different gauge and pulse shape to describe the effect of the laser pulse on the molecule. The present calculation provided us therefore with a useful check of the accuracy of our calculations. The results for the TDCSs, obtained when proper care is taken to account for the difference in the pulse shapes [23,25], are shown in Fig. 5, and are quite close to our previous results and results of other authors.

More to the point of the present paper, we see a structure in TDCSs in the vicinity of $\theta = 100^\circ$. The subtle interplay of relative phases of various components of the partial wave

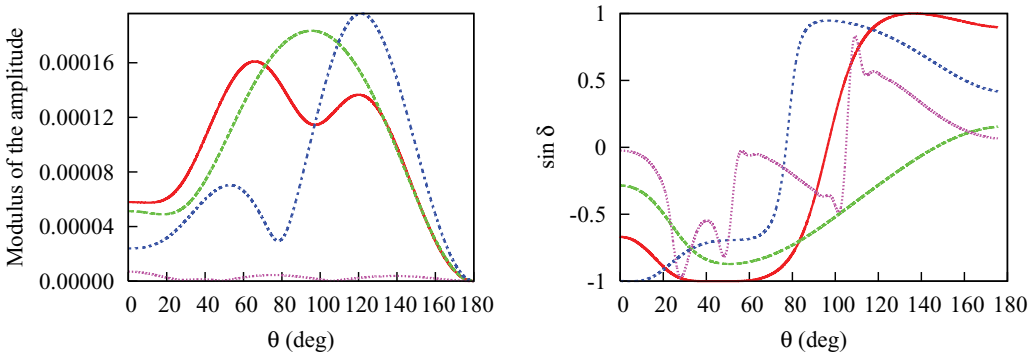

FIG. 4. (Color online) Contributions of the partial waves with $J = 1$ (green), dashed line, $J = 3$ (blue), short dashed line, and $J = 5$ (magenta), dots, to the ionization amplitude. Left panel- moduli of the amplitudes. Right panel: sines of the phases. Solid (red) line shows results for the total amplitude.

expansion for the amplitude is responsible for the appearance of this structure. Peculiarities in the dependence of the time delays as functions of the relative angle θ helped us to elucidate the origin of this phenomenon.

We considered above two instances when time delays as functions of the angle θ exhibit unusual behavior. In the region near $\theta \approx 100^\circ$ overall phase of the amplitude varies fast, leading to rapid variation of the time delays. For θ approaching the kinematic node at $\theta = 180^\circ$, the effect of the divergence of the time delays as functions of θ comes into play. This effect, as one can see from Fig. 3, is quite significant already for $\theta \approx 130^\circ$.

From the data presented in Fig. 5 we see that present results differ from the results of other authors and our previous results by no more than 10% . We can adopt this figure as an accuracy estimate of the present calculation. This estimate is perhaps too conservative, since the pulse shape we used in the present calculation differs from that used by other authors to obtain results shown in Fig. 5. We can expect the effects introduced by a particular pulse shape to vanish completely for a very long laser pulse. For the pulse duration of eight optical cycles that we considered, there may still be effects introduced by a particular pulse shape, and we may expect therefore some minor differences in TDCSs due to the pulse shape effects.

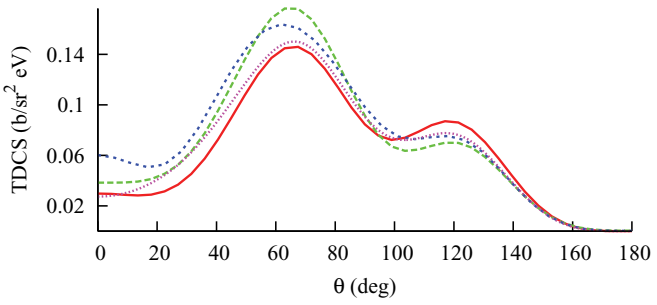

FIG. 5. (Color online) TDCSs for field and escape geometries considered in the paper, with $\boldsymbol{k}_1$ directed along the molecular axis and field directions, $\boldsymbol{k}_2$ in the perpendicular direction. Electron energies are $E_1 = E_2 = 12.2$ eV. Present calculation and our previous calculation [16] employing different gauges and pulse shapes are shown in (red) solid, and (green) dashed lines, respectively. (Blue) short dashed line: work [24]; (magenta) dots: results of the work [23].

Nevertheless, we can adopt the above-mentioned figure of 10% as an accuracy estimate of our calculation.

In both examples we considered above, time delays undergo considerable change, varying several times in magnitude. This variation exceeds by far the accuracy estimate we made above. We can be sure therefore that effects we reported for $\theta \approx 100^\circ$, and θ approaching the kinematic node at $\theta \approx 180^\circ$, are genuine physical effects. As for finer structures visible in Fig. 2 [such as small humps on the lower curve in the interval $\theta \in (80^\circ, 160^\circ)$], these may well be effects introduced by truncation of the partial wave expansion (2).

III. CONCLUSION

We studied angular dependency of the time delay in one-photon two-electron photoionization of the hydrogen molecule. We have shown that time delays as functions of the angle between velocities of the escaping electrons have poles at the points corresponding to the kinematic nodes of the reaction. In the vicinity of a pole the cross section is small; time delays, on the contrary, are large and are relatively easy to measure using attosecond streaking technique with the ionizing UV pump and a streaking IR probe. Eq. (9) tells us that study of the time delays in the vicinity of a pole can provide us with information about relative phases of the symmetric and antisymmetric amplitudes in the parametrized expression for the amplitude of the reaction.

We considered the simple case of the parallel field or molecule orientations and escape geometry with one electron escaping along the molecular axis. That was done so as not to obscure physics by unnecessary complications. Our results, in particular Eqs. (8) and (9), can be easily generalized for more complex geometries.

ACKNOWLEDGMENTS

The author would like to express his gratitude to Professor A. S. Kheifets for valuable discussions. The author is grateful to J. Colgan, K. Bartschat, and X. Guan for communicating their data in numerical form. Support of the Australian Research Council in the form of Discovery Grant No. DP0985136 is acknowledged. Facilities of the National Computational Infrastructure National Facility were used.

[1] P. B. Corkum and F. Krausz, Nature Phys. **3**, 381 (2007).
[2] A. Baltuška, T. Udem, M. Uiberacker, M. Hentschel, E. Goulielmakis, C. Gohle, R. Holzwarth, V. S. Yakovlev, A. Scrinzi, T. W. Hänsch *et al*., Nature (London) **421**, 611 (2003).
[3] R. Kienberger, E. Goulielmakis, M. Uiberacker, A. Baltuska, V. Yakovlev, and F. Bammer, Nature (London) **427**, 817 (2004).
[4] P. Eckle, A. N. Pfeiffer, C. Cirelli, A. Staudte, R. Dörner, H. G. Muller, M. Büttiker, and U. Keller, Science **322**, 1525 (2008).
[5] C. H. Zhang and U. Thumm, Phys. Rev. A **82**, 043405 (2010).
[6] J. C. Baggesen and L. B. Madsen, Phys. Rev. Lett. **104**, 043602 (2010).
[7] R. Pazourek, J. Feist, S. Nagele, and J. Burgdörfer, Phys. Rev. Lett. **108**, 163001 (2012).
[8] M. Schultze, M. Fieß, N. Karpowicz, J. Gagnon, M. Korbman, M. Hofstetter, S. Neppl, A. L. Cavalieri, Y. Komninos, T. Mercouris *et al*., Science **328**, 1658 (2010).
[9] S. Nagele, R. Pazourek, J. Feist, K. Doblhoff-Dier, C. Lemell, K. Takasi, and J. Burgdörfer, J. Phys. B **44**, 081001 (2011).
[10] D. Shafir, H. Soifer, B. D. Bruner, M. Dagan, Y. Mairesse, S. Patchkovskii, M. Y. Ivanov, O. Smirnova, and N. Dudovich, Nature (London) **485**, 343 (2012).
[11] O. Smirnova, V. S. Yakovlev, and M. Ivanov, Phys. Rev. Lett. **94**, 213001 (2005).
[12] I. A. Ivanov and A. S. Kheifets, Phys. Rev. A **83**, 063411 (2011).
[13] E. P. Wigner, Phys. Rev. **98**, 145 (1955).
[14] C. A. A. de Carvalho and H. M. Nussenzveig, Phys. Rep. **364**, 83 (2002).
[15] D. A. Varshalovich, A. N. Moskalev, and V. K. Khersonskii, *Quantum Theory of Angular Momentum* (World Scientific, Singapore, 1988).
[16] I. A. Ivanov and A. S. Kheifets, Phys. Rev. A **85**, 013406 (2012).
[17] T. J. Park and J. C. Light, J. Chem. Phys. **85**, 5870 (1986).
[18] A. S. Kheifets, I. A. Ivanov, and I. Bray, J. Phys. B **44**, 101003 (2011).
[19] A. S. Kheifets and I. A. Ivanov, Phys. Rev. Lett. **105**, 233002 (2010).
[20] I. A. Ivanov, Phys. Rev. A **83**, 023421 (2011).
[21] A. Huetz, P. Selles, D. Waymel, and J. Mazeau, J. Phys. B **24**, 1917 (1991).
[22] W. Vanroose, D. A. Horner, F. Martín, T. N. Rescigno, and C. W. McCurdy, Phys. Rev. A **74**, 052702 (2006).
[23] X. Guan, K. Bartschat, and B. I. Schneider, Phys. Rev. A **83**, 043403 (2011).
[24] J. Colgan (private communication).
[25] I. A. Ivanov and A. S. Kheifets, J. Phys. B **41**, 095002 (2008).